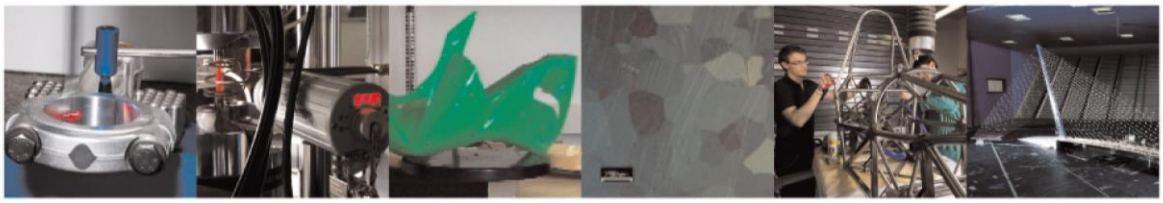

A comminution model with homogeneity and multiplication assumptions for the Waste Electrical and Electronic Equipment recycling industry

Diani, Marco; Pievatolo, Antonio; Colledani, Marcello; Lanzarone, Ettore

DIPARTIMENTO DI MECCANICA ■ POLITECNICO DI MILANO
via G. La Masa, 1 ■ 20156 Milano ■ EMAIL (PEC): pecmecc@cert.polimi.it
http://www.mecc.polimi.it
Rev. 0

A Comminution Model with Homogeneity and Multiplication Assumptions for the Waste Electrical and Electronic Equipment Recycling Industry

Marco Diani[1], Antonio Pievatolo[2],
Marcello Colledani[1], Ettore Lanzarone[2]

[1] *Politecnico di Milano, Department of Mechanical Engineering, Milan, Italy*
[2] *CNR-IMATI, Milan, Italy*

Abstract

Sustainable circular economy is introducing new industrial challenges, including recycling, to move from the *cradle-to-grave* paradigm to the innovative *cradle-to-cradle* concept. The core of several recycling systems consists of mechanical comminution, which aims at producing homogeneous mixtures of highly liberated particles. However, the complexity of comminution processes requires adequate models to control and optimize their behavior within the entire recycling system. In the literature, the so-called Population Balance Model has been proposed, which is however limited to the mining industry. In this paper, we examine the applicability of the Population Balance Models in the Waste Electrical and Electronic Equipment recycling industry. In particular, we include the *homogeneity* and *multiplication* assumptions, and analyze the impact of the comminution chamber saturation. These simplifications reduce the number of model parameters to be estimated, as the set of parameters remains the same over a wide range of working conditions. We tested our assumptions on a real system for recycling Printed Circuit Boards. Results showed the validity of the multiplication assumption and a marginal effect of saturation (p values for rotor velocity and saturation were always above 25% in an ANOVA with the Bonferroni correction). The homogeneity assumption is also tenable, with the exception of the initial transient, as the null hypothesis of constant output mass distribution under equivalent shredding times was never rejected at the 5% significance level. Outcomes of an out-of-sample validation confirmed the effectiveness of our simplified Population Balance Model (values of the Kolmogorov-Smirnov metric lower than 0.1).

Keywords: Recycling, Comminution Process, Multiplication Assumption, Homogeneity Assumption, Population Balance Model, Printed Circuit Boards

1. Introduction

The concept of Circular Economy was first proposed by Pearce and Turner (1989). Observing living systems, they suggested a similar approach for the industrial processes, in contrast with the classical linear economy model of *make - use - dispose*. The final goals are to reduce waste, avoid pollution, and create new adaptable and resilient productive systems. In particular, the new *cradle-to-cradle* paradigm, in contrast with the classical *cradle-to-grave* layout, pursues efficient and waste free systems, with consequent economic and environmental advantages (Braungart and McDonough, 2002). The idea is to move from classical linear economy to a new circular model, in which wastes re-enter as raw materials in a closed-loop (Ellen Mac Arthur Foundation, 2013).

Looking at the current waste production, Waste from Electrical and Electronic Equipment (WEEE) is the fastest-growing waste stream; for example, we may observe in Europe the 3-5% increase per year (Grübler, 2003). Moreover, WEEE includes several precious metals and rare earths, whose availability is reducing and cost is increasing. Thus, the development of sustainable (both from economic and environmental viewpoint) recycling systems and technologies to recover materials from WEEE is of fundamental importance for environment and high-tech products manufacturing (Ongondo et al., 2011).

Both mechanical and chemical processes can be adopted for recovering materials from WEEE. However, mechanical processes as comminution and separation represent the best alternative, because of the limited environmental impact, with low energy consumption and low production of by-products. They aim at producing homogeneous mixtures of highly liberated particles, where higher degrees of liberation are achieved by particles made of a small number of materials, and the highest possible liberation is obtained for particles made of only one material (Colledani and Tolio, 2013). In particular, it has been observed that lower particle sizes are associated with higher liberation rates (Oliveira et al., 2013).

In the literature, comminution processes are usually described by means of the so-called *Population Balance Model* (PBM). However, the available contributions are mainly related to the mining industry, while comminution models for recycling have attracted very limited attention so far. Size reduction processes used in material recycling substantially differ from those adopted in mining mainly for two reasons. First, processes in recycling systems are continuous, with a grate that regulates the flow rate and the dimensional distribution of the output, while in mining there are usually batch processes in a closed chamber. Second, material mixtures treated in recycling are more complex due to different parts joint and

welded together. These differences make the models developed for mining not suitable for recycling, or at least there is no contribution in the literature proving by experimental validation that they can be directly applied to recycling technologies (see Section 2 for references and details).

Moreover, PBMs and other comminution models require to estimate a set of parameters, which may vary with the working conditions. Thus, to move towards the industrial application of these models, to control and optimize the process within the entire recycling system, it is necessary to conduct a high number of preliminary experiments under different conditions, with loss of time and test material. This prevents the use of PBMs in the practice. The most important process parameters that affect the system are the rotor velocity, the chamber saturation, the characteristics of the input mass (e.g., the size distribution of the particles), the feed rate and the grate size.

In the light of these limitations, the goal of this work is twofold. On the one hand, we apply a PBM to a comminution system for recycling, to experimentally prove the applicability of PBMs in the recycling industry. On the other hand, we introduce some simplifying assumptions in order to use the same set of parameters over a wide range of working conditions, thus significantly reducing the number of experiments and allowing practical industrial application of PBMs. In particular, we introduce the so-called *homogeneity* and *multiplication* assumptions; moreover, we analyze whether the impact of the comminution chamber saturation on the process output can be neglected.

We model the comminution process considering several size classes and the stochastic evolution of particle mass distribution in these classes. The resulting stochastic process is characterized by a transition probability matrix, which determines the fraction of mass moving from any size class to a smaller one in a given time interval. In general, the process could be inhomogeneous, with a different transition matrix for each time interval. Moreover, the transition matrix could also depend on process parameters (e.g., the rotor speed and the grate size) and process conditions (e.g., the chamber saturation). The *homogeneity* assumption considers that the transition matrix does not depend on time, i.e., it is constant. The *multiplication* assumption consists of describing the evolution of particle mass distribution in the classes only in function of the number k of breakage intervals, rather than in function of elapsed time and rotor speed. We remark that, although the assumptions are discussed for a PBM, they are general and useful to simplify any other mathematical modelling of the comminution process.

Both the simplifying assumptions and the developed PBM including them are validated on a real comminution system. In particular, we consider a recycling system for Printed Circuit Boards (PCBs) for two reasons. On the one hand, PCBs are a relevant example of WEEE: they are at the basis of each modern electronic equipment, and they include a high amount of precious metals and rare earths. Typical values for metal content are summarized in Bizzo et al. (2014); the metallic fraction is between the 20% and the 40%, with high presence of copper (from about the 12% up to the 29% of the weight of the whole PCB), aluminum, iron and tin; moreover, relevant quantities of gold (from about 50 ppm up to 1000 ppm) and silver (from about 100 ppm up to 5000 ppm) are also present. On the other hand, PCBs are characterized by high variability of components, sizes, shapes, and are composed by a wide spectrum of materials. Thus, recycling PCBs is a very challenging task, which has not been effectively solved so far. Nowadays, advanced mechanical recycling approaches, based on feed-forward techniques, can recover up to the 95% of the metal fraction (depending on the element) only if properly liberated (Picone et al., 2016). However, this result can be achieved through a fine optimization of shredding parameters based on reliable models.

Our work fits into the idea of cleaner production because an optimized and controlled comminution process helps reducing WEEE and the consumption of energy and other resources required for the process. In other words, the comminutions process is a necessary brick for implementing the cradle-to-cradle paradigm and promoting a sustainable lifecycle of electrical and electronic equipments. Our work is also in line with the Industry 4.0 vision of manufacturing, in which smart and interconnected production systems optimize the complete chain. In fact, as largely documented in the literature, model-based systems engineering is a key enabler for such complex systems (Wortmann et al., 2017).

The rest of the paper is structured as follows. A literature review on WEEE recycling and mathematical models for size reduction comminution processes is presented in Section 2. Then, the structure of the proposed PBM for comminution in recycling and the simplifying assumptions are illustrated in Section 3. The experimental procedure for validating the assumptions and the simplified PBM are described in Section 4. Afterwards, the real recycling system for PCBs considered in this work is described in Section 5, and the results from validation are presented in Section 6. The conclusions of the work are drawn in Section 7. Finally, notations and abbreviations used in the paper are listed in the Appendix.

2. Literature review

The potential of reusing, recycling and remanufacturing WEEE is nowadays widely recognized in the literature. For example, Gu et al. (2016) recognized WEEE recycling as a key requirement to meet the resource demand of the electronics industry, by evaluating the sustainability of resource supply in different scenarios. Parajuly and Wenzel (2017) evaluated the benefits of circular economy (reuse and recycle), finding significant potential for reuse of different product types; however, they also highlighted that better WEEE management systems are needed to improve resource recovery. Zlamparet et al. (2017) proposed remanufacturing strategies and methods for reusing end-of-life products. Advantages are also highlighted from the environmental point of view. Menikpura et al. (2014) assessed the climate co-benefits of WEEE recycling, while Nelen et al. (2014) analyzed the benefits by considering a multidimensional indicator that involves several key aspects.

Size reduction processes seems to represent the best alternative for recycling WEEE (Cesaro et al., 2017). With respect to chemical processes, they require less energy and have a limited environmental impact, with low production of by-products (Colledani and Tolio, 2013). Moreover, size reduction processes are also at the basis of more complex treatment chains, which integrate mechanical and chemical processes. Their goal is to produce homogeneous mixtures of highly liberated particles, as low dimensional and liberated particles improve material recovery in downstream recycling processes (Schaik et al., 2004), together with other factors as a suitable product design (Schaik and Reuter, 2010).

Many attempts have been made to develop mathematical models that take into account both size reduction and liberation in mineral fields. Gaudin (1939) proposed a first liberation model based on the mineral texture, in which the liberation distribution of particles is predicted as a function of their size. Later, King (1979) proposed an equation to predict the linear liberation distribution as a function of particle size, while an analytical solution of the liberation problem for a batch grinding was proposed in King and Schneider (1998).

Several approaches determine the probability that the particles of a given class generate particles of another class, to model the particle distribution and its evolution along the comminution process. A possible approach is the so-called *Textural Modelling*, in which the size distribution evolution of mineral grain is inferred using mineralogical information. Gay and Wei (1999) and Gay (2004) proposed two approaches to solve this problem. The first is a mechanistic method in which the changes of composition distribution are direct consequence of ore properties. The latter is a probabilistic model based on entropy maximization

of probability subject to mass and composition constraints, i.e., the properties of the transformation matrix are inferred by examining the actual data without taking into account the mechanistic properties of the ore.

To the best of our knowledge, shredding in the recycling field has been only addressed in Schaik et al. (2004) and Castro et al. (2005). Schaik et al. (2004) modeled the relationship between product mineralogy and size reduction and liberation during the shredding of end-of-life vehicles, with the goal of maximizing material recovery. They also showed that breakage differs from that in traditional mineral processing, and illustrate the effect of product design on particle size reduction and liberation. Castro et al. (2005) presented a simulation model that describes the relationships between product design and liberation level, by simulating comminution and liberation phenomena as a function of product design. They applied the model to passenger vehicles and found that the principles used in classical mineral processing can be applied to describe comminution and liberation of end-of-life products during recycling, but they also showed that breakage of end-of-life products largely differs from that in natural minerals. Finally, they demonstrated that materials and joints can be chosen during product design in order to obtain the highest liberation and the lowest contamination during recycling.

The most effective approach to quantitatively describe comminution processes is given by the so-called *Population Balance Models* (PBMs). They represent the evolution of the particles by defining three quantities: the proportion of each particle type selected for breakage per unit of residence time; the degree to which each selected particle type undergoes breakage; the selection of particles removed from the process. PBMs are usually classified based on the mathematical treatment of time and space (Austin, 1971), which can be either discrete or continuous variables. Discrete-time PBMs have been mainly proposed because of the relatively short residence times of particles, and because the process can be described via a series of elementary breakage events, each one of short duration. Moreover, PBMs for comminution processes usually consider discrete particle sizes, because the experimental data are necessarily obtained in terms of discrete size classes. Looking at the structure of the models, linear PBMs assume the independence of particle breakage from the surrounding particle population.

A Discrete Linear PBM was originally developed by Broadbent and Calcott (1956), while a Time-Continuous Linear PBM by Sedlatschek and Bass (1953). More recently, Veroux and Grotti (2010) presented a discrete-time PBM that tries to combine both size reduction

and liberation aspects in a population balance framework. They defined particles made of fundamental discrete units, called atoms, which cannot be broken; moreover, these particles are assumed to be composed by two materials separated by a joint. Despite the novelty of the approach, practical applications and validations of this model are not reported.

Bilgili and Scarlett (2005) highlighted non-linear effects of particles in milling processes due to multi-particles interaction, describing three deviations from a linear behavior. First, an acceleration of breakage rate could be observed for mono-dimensional materials after long time; second, for binary materials, an increase of fine fraction could result in an increased breakage rate of larger materials; third, an addition of fine particles in the initial mass results in a decreased breakage rate. Following these results, Bilgili and Capece (2011) developed a PBM that includes non-linear effects due to particle-particle interactions, which results particularly useful for long time comminution process. This model considers mono-dimensional materials classified in different dimensional classes.

However, as mentioned by Schaik et al. (2004) and Castro et al. (2005), recycling is different from mineral comminution, and it is necessary to revisit the assumptions while adapting the existing models to the recycling industry. Thus, developing models tailored on WEEE is necessary to properly control and optimize their recycling processes. In particular, as all previous models require the estimation of a relevant number of parameters, tailoring the models to recycling would reduce their complexity and the number of required parameters, thus lowering the number and the cost of the experiments to estimate them. This is why we investigate the validity of some assumptions that may simplify the models for a future industrial application.

3. Comminution model and simplifying assumptions

In this section, we illustrate our comminution PBM and give a formal description of the simplifying assumptions. We also discuss the effect of the comminution chamber saturation. Finally, we show how the PBM can be employed to predict the output mixture distribution for any given input distribution, which is useful to control and optimize the process within the entire recycling system.

Before proceeding, we briefly describe the structure of a shredding machine for comminution. A common shredding machine includes a rotor with several cutting elements, arranged in such a way that the main breakage mechanisms in the shredding chamber are due to shear forces and friction. The material enters the chamber passing through a hopper, located in

the upper side of the machine, and is processed by the action of the rotating tools. During the permanence in the chamber, the material undergoes several breakages and its particles reduce their size. As soon as the particles get small enough to pass through the holes of a grate applied to the lower side of the chamber, they are discharged and collected in a bin placed at the bottom of the chamber. Different sizes of grate holes are used, based on the process; typical values are 4, 8 and 10 mm for coarse shredding, while 1 and 2 mm for fine shredding. The design of a typical shredding machine is reported in Figure 1.

3.1. Markovian comminution model

The structure of the proposed PBM follows the approach of Dehling et al. (2007), Section 7.4.3. We consider a discrete particle division into n size classes, where each class is indexed by i ($i = 1, \ldots, n$) and its size decreases with the index. The number n of classes is usually defined according to the measurement resolution that is available to analyze the mixture (see Section 5). We denote the overall mass of particles falling in class i at time t by $m_i(t)$ and we define $\mathbf{m}(t) = [m_1(t), \ldots, m_n(t)]^\top$.

We first present the comminution process and then the refilling and discharge process; finally, we combine them into the proposed PBM.

We consider a discrete-time process and denote by Δ the breakage interval, i.e., the smallest time interval in which a breakage of a particle may occur. Obviously, Δ depends on the type of rotor and its speed, in terms of revolutions per time unit. For example, if the rotor has three blades (one every 120 degrees) Δ is one third of the rotation period of the rotor, as each angle is traversed once by a blade during this interval.

As for the comminution, we consider:

- *Selection rate* S_{it}: mass fraction of particles in class i that are selected for breakage per time unit within the interval $[t, t + \Delta]$.
- *Breakage parameter* B_{ijt}: mass fraction of particles that, having left class i, go to class j in the interval $[t, t + \Delta]$.

Obviously, if $j \leq i$ then $B_{ijt} = 0$ because the mass that leaves class i is necessarily distributed over smaller size classes with $j > i$; moreover:

$$\sum_{j=i+1}^{n} B_{ijt} = 1 \quad \forall t.$$

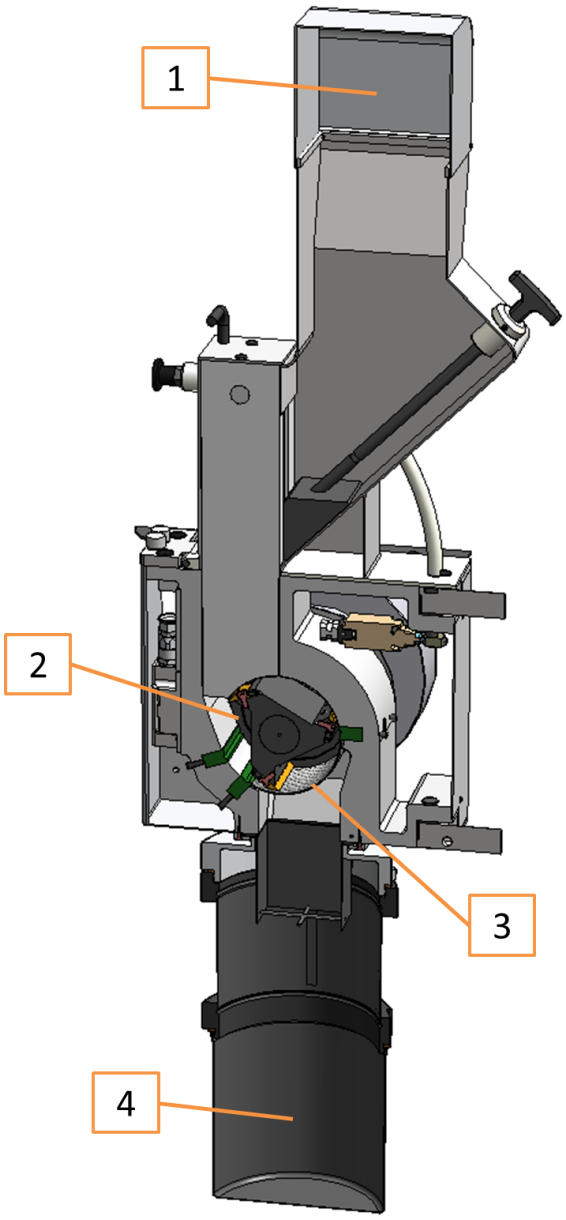

Figure 1: Design of a typical shredding machine: hopper (1), chamber (2), discharge grate (3), and bin (4).

With the given assumptions, the mass that leaves class i in a breakage interval $[t, t+\Delta]$ is given by $\Delta S_{it} m_i(t)$, and the corresponding mass that moves from class i to class $j > i$ is $m_{ij}(t+\Delta) = B_{ijt} \Delta S_{it} m_i(t)$.

Let us define by p_{ijt} the mass fraction that moves from class i to class j during a breakage interval $[t, t+\Delta]$. Thus,

$$p_{ijt} = \frac{m_{ij}(t+\Delta)}{m_i(t)} \quad \forall j > i, \qquad p_{iit} = 1 - \sum_{j=i+1}^{n} p_{ijt};$$

and S_{it} and B_{ijt} can be rewritten as follows:

$$S_{it} = \frac{1 - p_{iit}}{\Delta}; \qquad B_{ijt} = \frac{p_{ijt}}{1 - p_{iit}}.$$

We may now express $m_j(t+\Delta)$ as the sum of the mass remaining in class j from the previous time instant t and the collection of contributions from all larger size classes to class j:

$$\begin{aligned} m_j(t+\Delta) &= (1 - \Delta S_{jt}) m_j(t) + \sum_{i=1}^{j-1} m_{ij}(t+\Delta) = \\ &= p_{jjt} m_j(t) + \sum_{i=1}^{j-1} p_{ijt} m_i(t) = \sum_{i=1}^{j} p_{ijt} m_i(t) \end{aligned} \tag{1}$$

After placing all of the elements p_{ijt} in a matrix

$$\mathbf{P}_t^\top = \begin{bmatrix} p_{11t} & p_{12t} & \cdots & p_{1nt} \\ 0 & p_{22t} & \cdots & p_{2nt} \\ \vdots & \ddots & \ddots & \vdots \\ 0 & \cdots & 0 & p_{nnt} \end{bmatrix}$$

the particle mass evolution from time t to $t+\Delta$ can be rewritten in vectorial form as:

$$\mathbf{m}(t+\Delta) = \mathbf{P}_t \, \mathbf{m}(t). \tag{2}$$

We now include the refilling and discharge process in the model. The mass distribution $\mathbf{m}(t)$ processed from time t to $t+\Delta$ is given by two contributions, i.e., the mass $\mathbf{m}_{ch}(t)$ remaining in the chamber at time t and the mass $\mathbf{m}_{in}(t)$ refilled at time t. Thus:

$$\mathbf{m}(t+\Delta) = \mathbf{P}_t \, \mathbf{m}_{ch}(t) + \mathbf{P}_t \, \mathbf{m}_{in}(t). \tag{3}$$

In its turn, $\mathbf{m}_{ch}(t)$ is the mass remaining in the chamber after a part $\mathbf{m}_{out}(t)$ of $\mathbf{m}(t)$ has been discharged between $t - \Delta$ and t. This discharge process is regulated by another transition matrix $\mathbf{D}_t$ and the process is assumed to be linear:

$$\mathbf{m}_{ch}(t) = (\mathbf{I} - \mathbf{D}_t)\,\mathbf{m}(t); \tag{4}$$

$$\mathbf{m}_{out}(t) = \mathbf{D}_t\,\mathbf{m}(t). \tag{5}$$

where $\mathbf{D}_t$ is the diagonal discharge matrix at time t, and $\mathbf{I}$ denotes the identity matrix. The elements d_{iit} on the diagonal of $\mathbf{D}_t$ represent the fraction of mass $m_i(t)$ in class i that leaves the chamber.

The considered PBM is Markovian, because $\mathbf{P}_t^\top$ and $\mathbf{D}_t$ are actually two transition matrices and the state $\mathbf{m}(t + \Delta)$ at time $t + \Delta$ only depends on the state $\mathbf{m}(t) = \mathbf{m}_{ch}(t) + \mathbf{m}_{in}(t)$ at time t.

3.2. Formalization of the assumptions

The assumptions and the saturation effect are described in the PBM framework, although they can be formulated for the process without reference to any specific model.

We remark that, when including the discharge process and the matrix $\mathbf{D}_t$, the matrix $\mathbf{P}_t$ may change. However, we consider that, if the assumptions and the saturation effect are valid without discharge, they also hold when the discharge grate is included. Thus, we refer to model (2).

- ***Multiplication assumption***

  The output size distribution only depends on the number of breakage intervals, regardless of the pair rotor speed v and shredding time τ that generates that given number of breakage intervals.

  To illustrate, suppose that the process is running at speed v (expressed in revolutions per minute [rpm]). The breakage frequency (expressed in Hz) is given by $\frac{Nv}{60}$, where N is the number of blades in the rotor, and the breakage interval Δ is the inverse of such frequency. Thus, after τ seconds, the material has undergone

  $$k = \frac{\tau}{\Delta} = \tau\frac{Nv}{60} \tag{6}$$

  breakage intervals. The multiplication assumption states that the output size distribution only depends on k, i.e., it is the same for all pairs (v, τ) such that the product $v \times \tau$ is constant.

Under this assumption, the mass vector and the transition matrix are no longer indexed by the calendar time but by the index k of breakage events, i.e., $\mathbf{m}(t)$ becomes $\mathbf{m}(k)$ and $\mathbf{P}_t$ becomes $\mathbf{P}_k$, with $t = k\Delta$ for any integer k.

Given an initial mass distribution $\mathbf{m}(0)$, the mass distribution $\mathbf{m}(k)$ after k breakage events is given by a repeated application of the evolution equation (2):

$$\mathbf{m}(t) = \mathbf{m}(k\Delta) = \mathbf{P}_{(k-1)\Delta}\mathbf{P}_{(k-2)\Delta}\ldots\mathbf{P}_{\Delta}\mathbf{P}_0\,\mathbf{m}(0)$$

whatever the values of v and τ are. Obviously, k will correspond to different calendar times t based on v and τ.

- ***Homogeneity assumption***

  The transition matrix $\mathbf{P}_h$ does not depend on h, i.e., $\mathbf{P}_h = \mathbf{P}$ independently of h, where h either denotes the calendar time t or the number of breakage events k. Thus, the comminution process does not depend on how long the rotor was previously running.

These assumptions, if valid, simplify the structure of any comminution model. Thus, they reduce the amount of parameters to be estimated and, consequently, the number of experiments required to train the model. In particular, thanks to the multiplication assumption, the experimental results obtained with a given rotor speed v are also representative of other speeds. This is a relevant advantage for the industrial practice, where each new pair of WEEE type and shredder machine requires a customization of model parameters.

In the case of the PBM in (2), the process is entirely characterized by the constant transition matrix $\mathbf{P}$, and the output size distribution has the following very simple expression:

$$\mathbf{m}(\Delta) = \mathbf{P}\mathbf{m}(0); \tag{7}$$

$$\mathbf{m}(t) = \mathbf{m}(k\Delta) = \mathbf{P}^k\mathbf{m}(0); \tag{8}$$

where the transition matrix estimated at a given speed can predict the output also at different untested speeds.

When referring to the complete PBM with discharge in (3)-(5), we also assume the discharge matrix to be homogeneous and the assumptions lead to the following form:

$$\mathbf{m}(k+1) = \mathbf{P}\,\mathbf{m}_{ch}(k) + \mathbf{P}\,\mathbf{m}_{in}(k); \tag{9}$$

$$\mathbf{m}_{ch}(k) = (\mathbf{I} - \mathbf{D})\,\mathbf{m}(k); \tag{10}$$

$$\mathbf{m}_{out}(k) = \mathbf{D}\,\mathbf{m}(k). \tag{11}$$

- ***Saturation effect***

  Saturation Sat is defined as the ratio between the material volume within the chamber and the chamber capacity. If different saturation levels do not determine different comminution processes, the experiments to train the model are reduced, as the experiments conducted at a given Sat are significant also for other saturations. Moreover, when Sat does not affect the process, the comminution throughput can be easily changed by simply varying Sat (within operable limits) without impacting the output size distribution. Otherwise, in case Sat affects the comminution processes, not all throughputs could be set while maintaining the desired output size distribution.

4. Experimental procedure for validating the assumptions and the simplified PBM

We first present the experiments to validate the assumptions and analyze the impact of saturation. Then, we describe the experiments to validate the PBM that incorporates the proposed simplifications.

We remark that the experiments for the assumptions are independent of the PBM, as they can be adopted for any modeling approach to WEEE comminution. In particular, in the experiments of Section 4.1, we test them with closed chamber experiments. Then, the entire simplified PBM in (9)-(11) is considered in Section 4.2.

4.1. Assumptions

The multiplication assumption and the impact of the saturation assumption are jointly tested through the following experiments. Three pairs of speed and shredding time (v, τ) are selected with a constant number k of breakage intervals equal to 2400, i.e., $\tau \frac{Nv}{60} = 2400$; see (6). Then each pair (v, τ) is run with three Sat levels. The resulting 9 experimental conditions, with $N = 3$ (see Section 5), are reported in Table 1. Equal mixture distributions $\mathbf{m}(0)$ are taken for all experiments. Thus, equal output distributions $\mathbf{m}(\tau)$ for experiments in the same row of Table 1 indicate the absence of Sat effect, while equal distributions $\mathbf{m}(\tau)$ in a column support the multiplication assumption.

The homogeneity assumption is tested as follows. Starting from a given input mixture distribution $\mathbf{m}(0)$, the comminution process is run for a time σ; then, the process is stopped and restarted from $\mathbf{m}(\sigma)$ for another time τ. If homogeneity holds, the final output size distributions $\mathbf{m}(\sigma + \tau)$ of all runs with the same value of $\sigma + \tau$ should be the same for any

		Sat		
		25%	50%	75%
(v, τ)	1200 rpm - 40 sec	Exp 40-25	Exp 40-50	Exp 40-75
	2000 rpm - 24 sec	Exp 24-25	Exp 24-50	Exp 24-75
	2400 rpm - 20 sec	Exp 20-25	Exp 20-50	Exp 20-75

Table 1: Experimental conditions for testing the multiplication assumption and the saturation effect. Experiments are labelled by the values of duration (in seconds) and saturation (in percentage).

Shredding time	$\sigma + \tau = 60$			$\sigma + \tau = 75$		
[seconds]	Comb. 1	Comb. 2	Comb. 3	Comb. 1	Comb. 2	Comb. 3
σ	60	15	30	75	45	60
τ	0	45	30	0	30	15

Table 2: Two-phase shredding experiments for the homogeneity assumption: three combinations with $\sigma+\tau = 60$ and three with $\sigma + \tau = 75$, each one repeated three times.

pair of σ and τ. In particular, experiments are run at $v = 1200\,rpm$ with two different values of $\sigma + \tau$. For each value of $\sigma + \tau$, we analyze three combinations, always starting from the same distribution $\mathbf{m}(0)$ and the same Sat. Finally, three replicates are performed for each combination, to reduce the variance of $\mathbf{m}(\sigma + \tau)$. The overall experimental scheme is reported in Table 2.

4.2. Simplified PBM

In this section we describe the procedure to estimate the PBM parameters, and then the conducted experiments.

The estimation procedure of $\mathbf{P}$ and $\mathbf{D}$ is based on the following experimental limitations:

- It is possible to measure only $\mathbf{m}_{in}(k)$ and $\mathbf{m}_{out}(k)$.
- It is not possible to observe the mass distribution in the chamber, while the total mass inside the chamber can be computed using the input, the output and the initial mass.
- Matrices $\mathbf{P}$ and $\mathbf{D}$ refer to a time interval during which it is possible to observe $\mathbf{m}_{in}$ and $\mathbf{m}_{out}$ in practice, in such a way that the output mass is actually affected by the input mass and physical measurement constraints are met.

The estimation is performed by minimizing the difference between the experimentally observed output mass distribution and that obtained from the model. In particular, we minimize the following quantity

$$\min_{\mathbf{P},\mathbf{D}} \sum_{k=1}^{k^*} \|\mathbf{m}_{out}^{obs}(k) - \mathbf{m}_{out}(k)\|_2, \tag{12}$$

where $\mathbf{m}_{out}^{obs}(k)$ is the experimentally observed output mass distribution at k, and $\mathbf{m}_{out}(k)$ is the corresponding distribution obtained from the model in function of $\mathbf{P}$ and $\mathbf{D}$.

The latter is obtained by iterating model equations (9)-(11):

$$\mathbf{m}_{out}(k) = \mathbf{D} \sum_{\iota=0}^{k-1} [\mathbf{P}(\mathbf{I} - \mathbf{D})]^{k-\iota+1} \mathbf{P}\mathbf{m}_{in}(\iota) \qquad k = 1, 2, \ldots$$

which relates the input mass $\mathbf{m}_{in}$ at all time steps up to $k-1$ to the output at time step k.

With n size classes, there are $\frac{1}{2}[n + n(n-1)] = \frac{1}{2}n(n+1)$ unknown model parameters; n of them are the entries of the diagonal of $\mathbf{D}$, and the remaining ones the entries of $\mathbf{P}$.

The minimization of (12) is numerically obtained with the function *fmincon* of Matlab. We consider in the optimization the logit value of the probabilities:

$$q_{ij}^p = log\frac{p_{ij}}{1 - p_{ij}} \quad \text{and} \quad q_{ii}^d = log\frac{d_{ii}}{1 - d_{ii}};$$

thus, it is automatically guaranteed that all entries p_{ij} and d_{ii} are between 0 and 1. Moreover, we impose that the entries d_{ii} are not decreasing with i, as the probability is higher for smaller classes. Due to the presence of local optima, the minimization is repeated with 30 different initializations.

Analyses were conducted for $2mm$ and $4mm$ grate size. PBM parameters were estimated with 6 consecutive sampling intervals, with a constant input flow of 4.56 g/s, equal sampling intervals of 15 seconds, and speed v of $1200rpm$. A first in-sample analysis and a second out-of-sample validation were conducted. For the in-sample analysis, we compared the model outcomes with the same data used to estimate model parameters; for the out-of-sample validation, we considered data from 11 consecutive sampling intervals of 10 seconds (under constant input flow of 6.84 g/s and speed v of 1800 rpm) and compared the mass distributions of the last 4 intervals.

5. Application to a real PCB shredding system

We applied our framework to a real system for PCB recycling. We studied the Re/Demanufacturing pilot plant of the Institute of Intelligent Industrial Technologies and Systems

for Advanced Manufacturing, National Research Council of Italy, Milan, Italy (website of STIIMA). The pilot plant is divided into three cells:

- *Cell 1* dedicated to the semi-automated disassembly of mechatronics products;
- *Cell 2* focused on testing and repair (if possible and economically sustainable) of end-of-life PCBs;
- *Cell 3* devoted to recover materials, e.g., precious metals, from non-repairable PCBs. PCBs undergo two different shredding stages, with a single shaft shear shredder for coarse comminution (first stage) and a cutting mill for fine pulverization (second stage). Finally, liberated metal particles are separated from non-conductive particles through a Corona Electrostatic Separator.

We considered the second-stage shredding process, which takes places in the Cutting Mill SM300 (Retsch, Düsseldorf, Germany), a typical shredding machine. It includes a rotor with 3 cutting elements per blade ($N = 3$) and 6 stacked blades, with a total of 18 cutting elements. It has a cylindrical chamber, with a diameter of 13 cm and a height of 13 cm, while the diameter of the rotor is equal to 9 cm. The picture of the SM300 and a particular of its rotor are reported in Figure 2.

Input and output particle-size distributions for the experiments related to the assumptions were measured by means of an analytic sieve. We adopted the AS200 (Retsch, Düsseldorf, Germany), depicted in Figure 3, which divides the material into 9 classes ($n = 9$); see Table 3. As for the experiments related to the simplified PBM, distributions were characterized using the computerized particle analyzer CPA 2-1 (Haver & Boecker, Oelde, Germany), which performs high speed (quasi real-time) dimensional distribution and shape analysis on particles from 34 μm up to 25 mm.

As mentioned, batch experiments for validating the assumptions were performed without mass discharge from the chamber. Ideally, these experiment require the comminution chamber to be closed, without a discharge grate. However, a completely closed grate cannot be used, due to thermal power generation during shredding, which must be dissipated. Otherwise, the internal temperature of the chamber would increase too much. Thus, a grate of 0.25 mm was used for the batch experiments, to enable thermal dissipation while minimizing particle discharge. Such an adjustment had marginal impact on the experiments, as a very small fraction of material left the chamber; moreover, the particles that left the chamber were in the smallest size class ($i = 9$), which does not undergo measurable transitions.

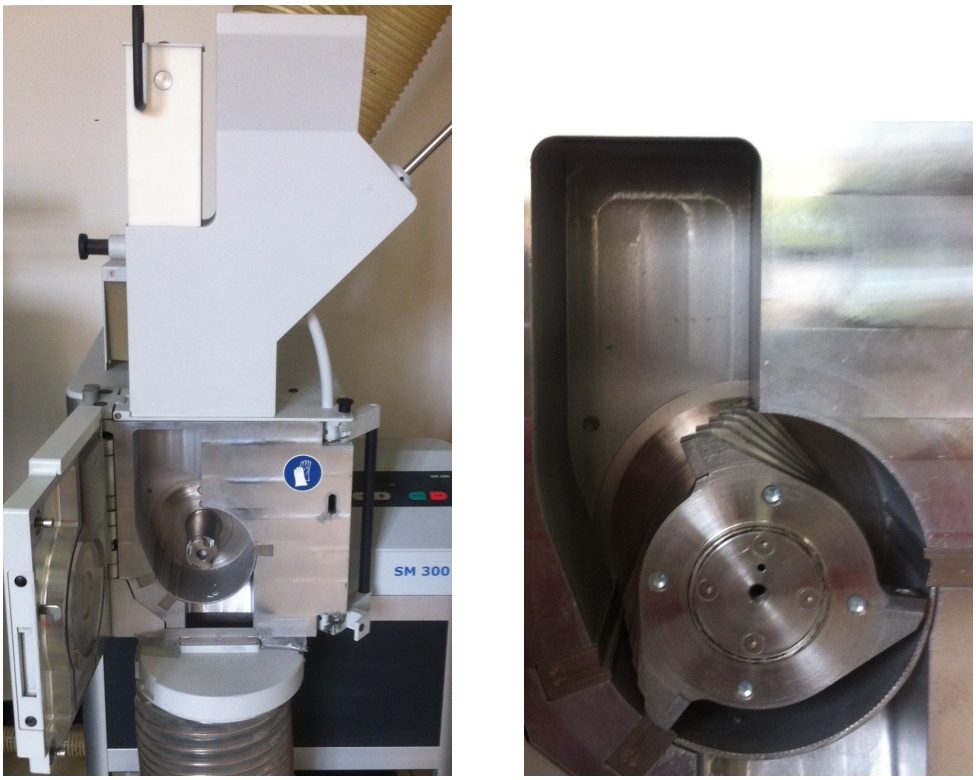

(a) (b)

Figure 2: Cutting Mill SM300: machine (a) and rotor (b).

Size class	Size [mm]	
i	Lower bound	Upper bound
1	4	∞
2	2.5	4
3	2	2.5
4	1.4	2
5	1	1.4
6	0.71	1
7	0.4	0.71
8	0.2	0.4
9	0	0.2

Table 3: Size classes measured by the adopted sieve (lower and upper bound for each class).

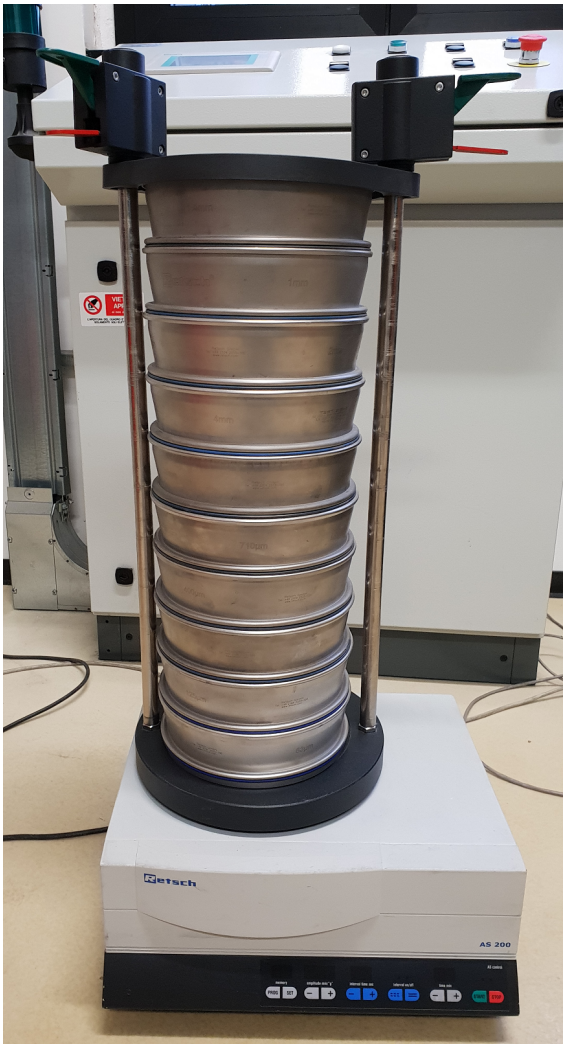

Figure 3: Analytic sieve AS200.

All samples were obtained from real end-of-life PCBs: as for the assumptions, from cockpit PCBs from Magneti Marelli (Corbetta, MI, Italy) and washing machine PCBs from Candy (Brugherio, MB, Italy); as for the simplified PBM, from a mix of PCBs coming from computers and screens. In both cases, samples were pre-shredded together with the first-stage shredding machine, thus obtaining a coarse particle mix. Then, to get the desired mass distributions, the mix was divided into the nine required size classes with the analytic sieve and the particles of the different classes were combined following the required proportions. An example of initial sample is depicted in Figure 4.

The amount of material to be employed with the considered shredding machine was determined based on the mass m_{sat} at $Sat = 100\%$. It is given by $m_{sat} = \rho V$, where ρ is the density of the particle mix and V the empty volume of the shredding chamber, which is given by the whole volume of the chamber minus the volume of the blades. The measured values were $\rho = 0.75\ g/cm^3$ (for both assumptions and PBM experiments) and $V = 330\ cm^3$, thus giving $m_{sat} = 247.5\ g$

6. Results

We first show the outcomes from the analysis of the multiplication assumption together with the saturation effect. Then, we consider the homogeneity assumption together with a revisitation required by the results. Finally, we validate the proposed PBM. The results presented in Sections 6.1 and 6.2 have been obtained using R (R Core Team, 2014), while those in Section 6.3 using Matlab.

6.1. Multiplication assumption and saturation effect

Table 4 shows the percentages of $\mathbf{m}_{out}$ in each size class for the nine experiments with the same number $k = 2400$ of breakage intervals (see Table 1). In addition, the output size distributions are displayed in Figure 5; plots on a row have the same (v, τ) pair, while plots on a column the same Sat.

On a first qualitative evaluation, the distributions look broadly similar. However, on examining single size classes, variations that might not be due to randomness can be observed. For example, the mass leaves the largest size class more easily when both v and Sat take low values, such as $(1200, 25\%)$, $(1200, 50\%)$ and $(2000, 25\%)$. To assess if v and Sat have a significant effect, a two-way ANOVA model with v and Sat as main (categorical) effects was fitted to the data in each size class, using the weight of the output material in that

(a)

(b)

Figure 4: Example of initial sample: mixed (a) and divided into size classes (b).

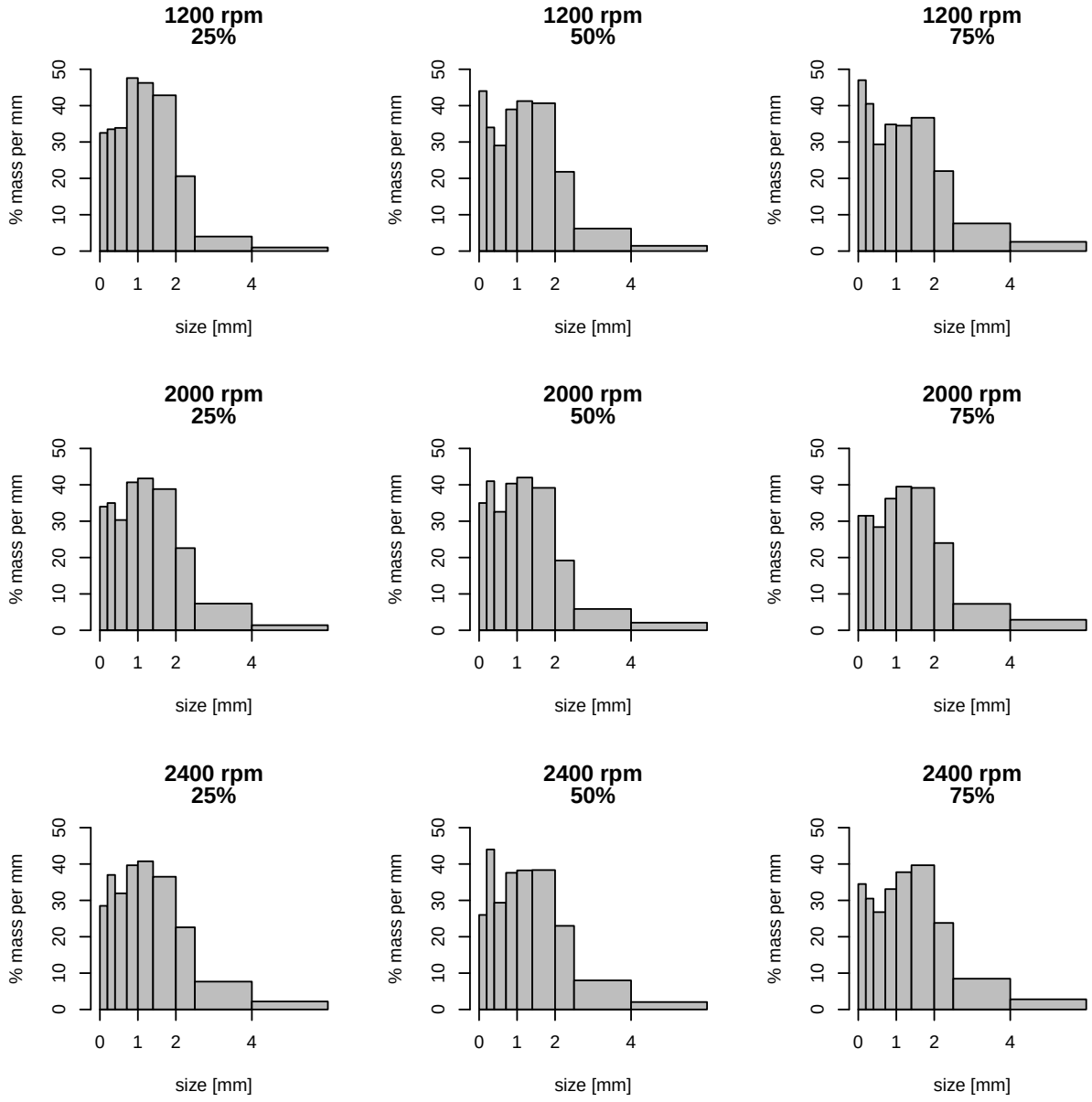

Figure 5: Histograms of the $\mathbf{m}_{out}$ distributions by v and Sat, based on the data in Table 4. Each column refers to a size class whose height is the percentage of mass in the class divided by the class width (limited to 6 mm for $i = 1$).

Sat		Size class i								
(%)	Experiment	9	8	7	6	5	4	3	2	1
25	Exp 40-25	6.5	6.7	10.5	13.8	18.5	25.7	10.3	6.0	2.0
	Exp 24-25	6.8	7.0	9.4	11.8	16.7	23.3	11.3	11.0	2.8
	Exp 20-25	5.7	7.4	9.9	11.5	16.3	21.9	11.3	11.5	4.4
50	Exp 40-50	8.8	6.8	9.0	11.3	16.5	24.4	10.9	9.3	2.9
	Exp 24-50	7.0	8.2	10.1	11.7	16.8	23.5	9.6	8.8	4.2
	Exp 20-50	5.2	8.8	9.1	10.9	15.3	23.0	11.5	12.0	4.1
75	Exp 40-75	9.4	8.1	9.1	10.1	13.8	22.0	11.0	11.4	5.1
	Exp 24-75	6.3	6.3	8.8	10.5	15.8	23.5	12.0	10.9	5.8
	Exp 20-75	6.9	6.1	8.3	9.6	15.1	23.8	11.9	12.7	5.6

Table 4: Fraction [%] of $\mathbf{m}_{out}$ in each size class for the nine experiments of multiplication assumption and saturation effect.

class as response. The $F(4,4)$ statistics for testing this model against the model with no effects has been reported in Table 5, together with the associated class-by-class p values and the family-wise corrected p values. Each corrected p value was obtained by applying the Bonferroni correction for multiple testing (i.e., multiplying each individual p value by 9). Results show that, even considering non-corrected p values, *Sat* and v are significant only at the 5% level for the largest class $i = 1$ and at the 10% level for the class $i = 6$. This is in agreement with Figure 5, where the only stable changing patterns of column height appear in the largest class and, to a lesser extent, in class $i = 6$ (0.71–1 *mm*, fourth column from the right). Considering the corrected p values, *Sat* and v are never significant.

A closer look at the individual models for size classes $i = 1$ and $i = 6$ is provided by the ANOVA tables in Table 6, where only *Sat* appears to be significant at the 5% level. However, according to the corrected p values, the null hypothesis is never rejected at the 10% level, and no factor is highly significant for the entire $\mathbf{m}_{out}$ distribution. Thus, based on our data, we can affirm that the multiplication assumption is not rejected and saturation has little effect.

6.2. Homogeneity assumption

We tested the hypothesis that the expected mass fraction in each class is the same if $\sigma + \tau$ is constant.

Size class i	$F(4,4)$ statistics	p value	Corrected p value
9	2.416	0.207	>1
8	0.470	0.759	>1
7	1.816	0.289	>1
6	4.591	0.085	0.765
5	1.882	0.278	>1
4	0.300	0.865	>1
3	1.257	0.415	>1
2	2.076	0.248	>1
1	9.083	0.028	0.252

Table 5: $F(4,4)$ statistics, p value and corrected p value from the ANOVA with two factors Sat and v and three levels for each factor.

Size class $i = 6$ (0.71–1 mm)

	Df	Sum	Sq Mean	Sq F value	Pr(>F)	
v	2	1.7422	0.8711	1.6505	0.30016	(a)
Sat	2	7.9489	3.9744	7.5305	0.04404	*
Residuals	4	2.1111	0.5278			

Size class $i = 1$ (> 4 mm)

	Df	Sum	Sq Mean	Sq F value	Pr(>F)	
v	2	2.9267	1.4633	4.2829	0.10133	(b)
Sat	2	9.4867	4.7433	13.8829	0.01586	*
Residuals	4	1.3667	0.3417			

Table 6: Two-way ANOVA tables for size classes $i = 6$ (a) and $i = 1$ (b) versus v and Sat. Symbol * denotes statistical significance, i.e., a p value lower than 0.05. The ANOVA tables of the other size classes show no significant effects.

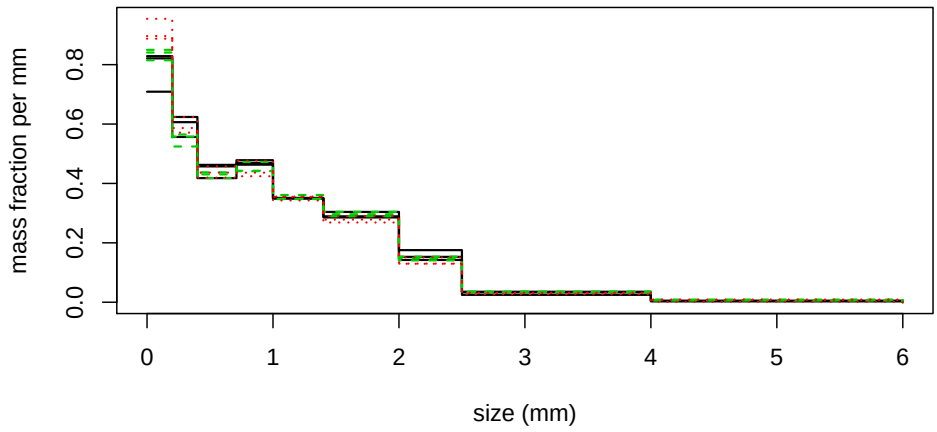

(a)

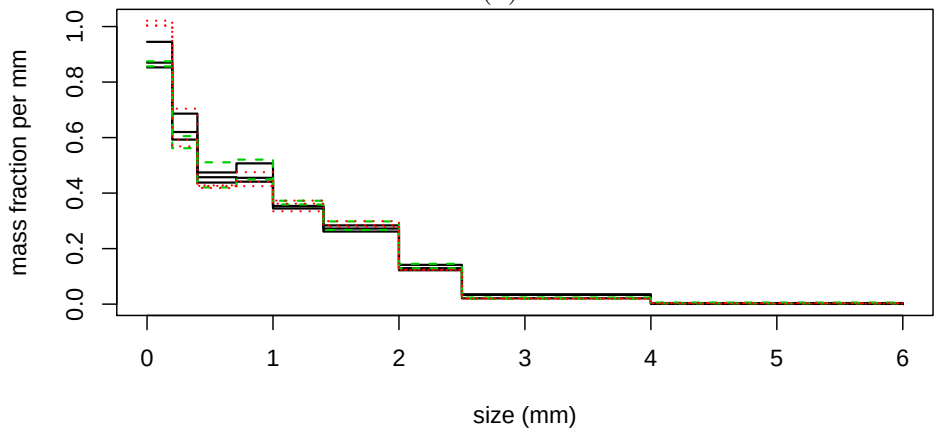

(b)

Figure 6: Particle size histograms for the homogeneity experiments: experiments with $\sigma + \tau = 60$ (a) and with $\sigma + \tau = 75$ (b). Curves in the same color represent the same condition, and different line types represent replication.

Three replications were performed for each pair (σ, τ) (see Table 2), which gave limited variance of the error. Results in terms of the measured weights for each class are reported in Table 7 for each replication. Based on Table 7, size class distributions were then computed by dividing each weight by the width of the class and by the total weight; the resulting distributions are displayed in Figure 6. It can be noticed that the output size distributions are similar to each other for both $\sigma + \tau = 60$ and $\sigma + \tau = 75$, and the observed small variability among distributions seems to be inherent to process randomness and sieving variability rather than to a systematic effect of inhomogeneity, as colors and line types are shuffled.

Table 8 reports the individual p values of the ANOVA test for constant mean in every

Size	$\sigma+\tau=60$									$\sigma+\tau=75$								
class i	$60+0$			$15+45$			$30+30$			$75+0$			$45+30$			$60+15$		
1	1.0	0.9	0.2	0.5	0.3	0.5	0.6	0.9	0.9	0.2	0.4	0.4	0.4	0.2	0.1	0.9	0.6	0.3
2	2.7	2.7	2.3	2.7	2.0	2.9	2.7	2.9	2.9	1.7	1.7	1.7	2.6	1.6	2.7	1.9	1.9	1.6
3	3.7	4.3	3.7	4.7	4.1	3.9	4.0	3.9	4.2	3.5	3.5	3.5	3.7	3.3	3.1	3.4	3.9	3.5
4	9.5	9.9	9.2	9.3	9.2	10.0	9.6	10.1	9.5	9.8	10.1	9.5	8.9	8.0	8.3	8.9	9.6	8.7
5	7.8	8.1	8.1	7.5	7.5	7.7	7.8	7.7	7.6	8.3	8.4	7.6	7.4	7.2	7.0	7.5	8.0	7.8
6	7.2	7.0	7.9	7.2	7.3	7.6	7.4	7.1	7.0	7.9	7.2	7.0	6.9	7.5	6.5	7.3	7.0	8.2
7	7.7	7.4	8.1	7.6	7.7	7.1	7.0	7.5	7.3	7.6	7.3	7.5	7.1	7.5	7.2	8.4	7.0	8.6
8	7.1	6.5	6.7	6.5	6.7	6.1	6.1	5.8	6.1	6.8	6.4	8.0	6.2	7.0	6.3	—	6.5	6.1
9	10.2	10.1	10.9	7.6	8.9	9.0	8.8	9.4	9.2	11.5	11.3	11.6	9.1	8.7	9.6	—	9.2	9.5

Table 7: $\mathbf{m}_{out}$ weights [grams] for the homogeneity experiments ("—" refers to a missing measurement).

Size class i	$\sigma + \tau = 60$	$\sigma + \tau = 75$
1	0.32	0.41
2	0.36	0.13
3	0.23	0.26
4	0.13	0.45
5	0.92	0.51
6	0.35	0.53
7	0.56	0.34
8	0.15	0.64
9	0.04	0.01

Table 8: Class by-class p values, without Bonferroni correction, for testing the homogeneity assumption.

size class while keeping $\sigma + \tau$ fixed. By applying the Bonferroni correction for multiple testing of the nine classes (i.e., multiplying the p values by 9), the null hypothesis at the 5% significance level is never rejected. Hence, the homogeneity assumption is tenable, although the smallest size class $i = 9$ exhibits lower p values than the other classes. The reason for the larger variability of class $i = 9$ is in the way in which the experiments were conducted: since a completely closed grate could not be used, part of the finest material left the chamber; then, it was collected and sieved together with the material inside the chamber. This additional operation increased the variability of the smallest size class.

6.2.1. Homogeneity assumption, revisited

All experimental runs of the previous section lasted for at least 15 seconds; thus, possible inhomogeneities in the initial shredding period, with coarser input mixture, cannot be detected with the considered data. At the same time, it is not feasible to further reduce this time interval in practice.

However, the evolution equation (8) offers a further possibility of verification. Under the homogeneity and multiplication assumptions, the evolution from breakage interval $k-1$ to k is written as:

$$m_i(k) = \sum_{j=1}^{i} p_{ji} m_j(k-1) = \sum_{j=1}^{i} p_{ji} \left\{ \sum_{l=1}^{j} p_{lj} m_l(k-2) \right\} \qquad i = 1, \ldots, n, \quad k \geq 2$$

Thus:

$$\frac{m_i(k)}{m_i(k-1)} = \frac{\sum_{j=1}^{i} p_{ji} \left\{ \sum_{l=1}^{j} p_{lj} m_l(k-2) \right\}}{\sum_{j=1}^{i} p_{ji} m_j(k-2)} \qquad i = 1, \ldots, n, \;\; k \geq 2$$

This expression reduces to $m_1(k)/m_1(k-1) = p_{11}$ when $i = 1$; thus, if the model is valid, the mass fraction in the largest size class geometrically decreases with k. On the contrary, this reduction is not possible for smaller size classes. However, as the shredder runs, larger size classes get progressively empty, until all mass will end in the smallest class. Hence, for $i = 2$, there is a large enough value of k such that $m_1(k-2) = 0$, in which case it is easy to see that $m_2(k)/m_2(k-1) = p_{22}$, and so on for $i > 2$.

To experimentally verify that the ratios $m_i(k)/m_i(k-1)$ tend to p_{ii}, the mass should be characterized at extremely short time intervals without stopping the shredder, which is of course impossible. Instead, it is possible to perform a series of runs with the same input distribution, speed and saturation, and with durations that arithmetically increase, to evaluate ratios $m_i(k)/m_i(k-\delta)$, where the increment δ makes it possible to distinguish two runs. These experiments are already available, as the runs in Table 7 provide outputs at $\sigma =$ 15, 30, 45, 60 and 75 seconds. At 1200 rpm, the sampling interval of 15 seconds corresponds to $\delta = 900$ breakage intervals, so that we can compute the ratios are $m_i(k)/m_i(k-900)$. This fact does not change the verification method, which is still valid after replacing $\mathbf{P}$ by $\mathbf{P}^{900}$ and comparing the outputs of consecutive sampling intervals instead of consecutive breakage intervals.

Figure 7 shows the sequence of ratios for all size classes. Two features can be observed: all curves settle down at a constant value; curves show a very different ratio for the first sampling interval, when the machine is started with a much coarser mixture than the rest of the process. The largest classes (indexed by $i = 1$, $i = 2$ and $i = 3$) reach a value smaller than one, as expected, whereas the remaining classes would need a rather longer shredding time, because each of them is still receiving material from larger classes. Anyway, the behavior predicted by the model is observed, excluding the initial transient phase.

6.3. Simplified PBM

Results from the in-sample analysis are reported in Figures 8 and 8, where the experimentally observed output mass distribution $\mathbf{m}_{out}^{obs}(k)$ and the corresponding distribution $\mathbf{m}_{out}(k)$ obtained from the model are compared. They prove that, passing from the transient to the stationary state, a strong adherence between model and data is observed.

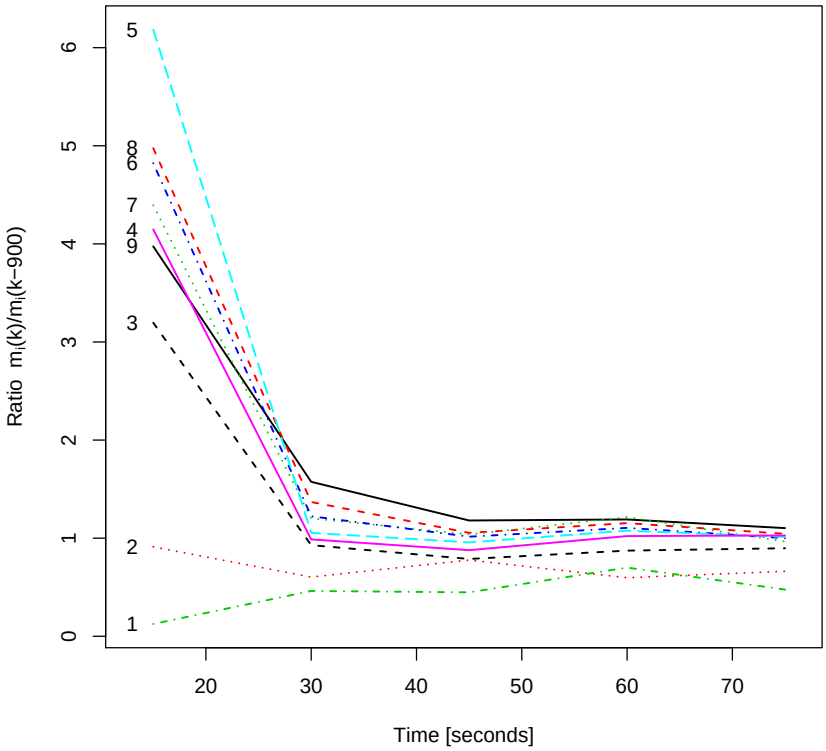

Figure 7: Ratios $m_i(k)/m_i(k-900)$ for each size class i; each line refers to a class, whose label is reported on the left of the plot.

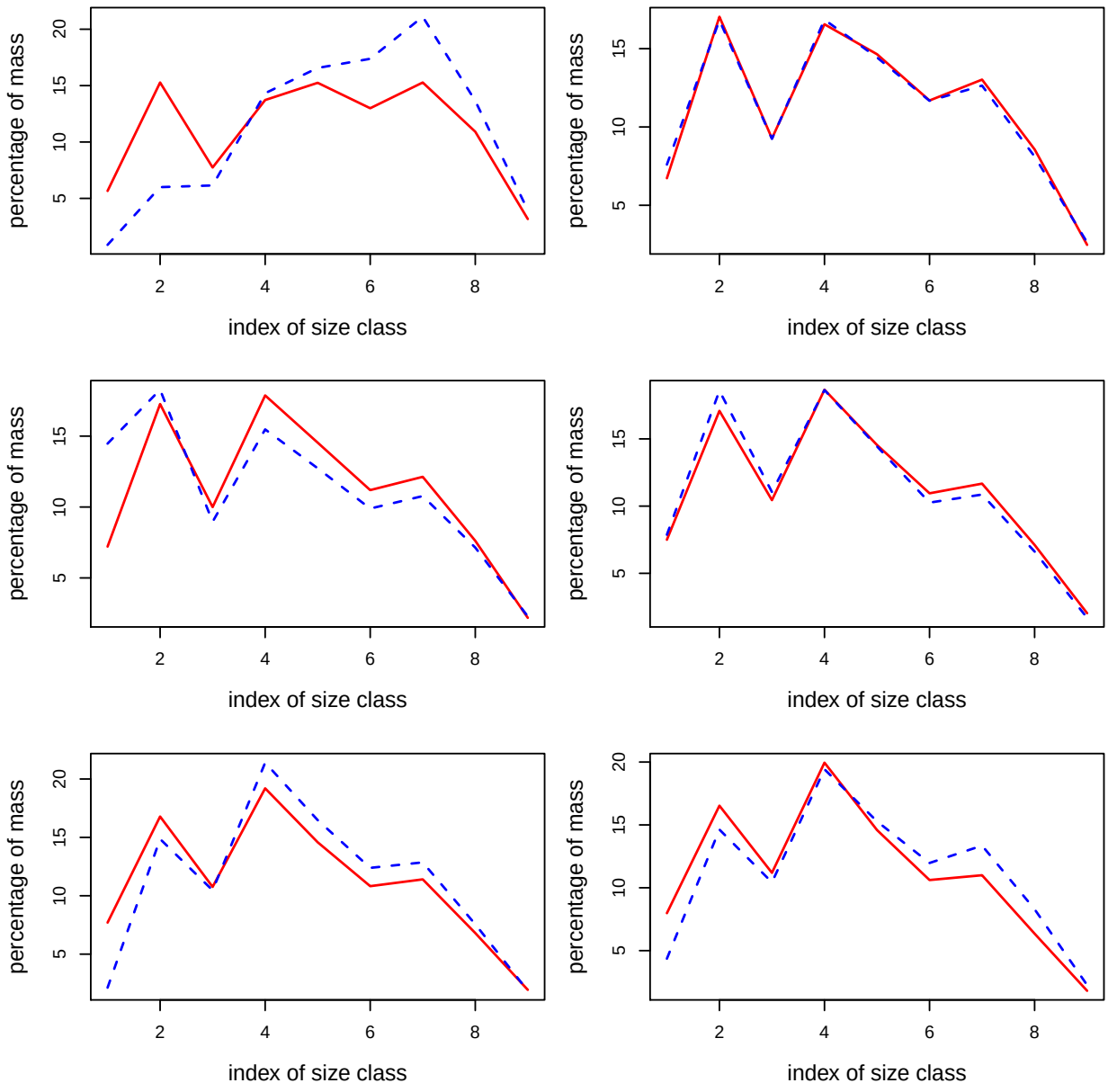

Figure 8: In-sample analysis for 2 mm grate size: observed data $\mathbf{m}_{out}^{obs}(k)$ (blue line) and model prediction $\mathbf{m}_{out}(k)$ (red line). Plots in each subfigure report the distributions for the 6 sampling intervals, by row, with increasing k from the top left to the bottom right corner.

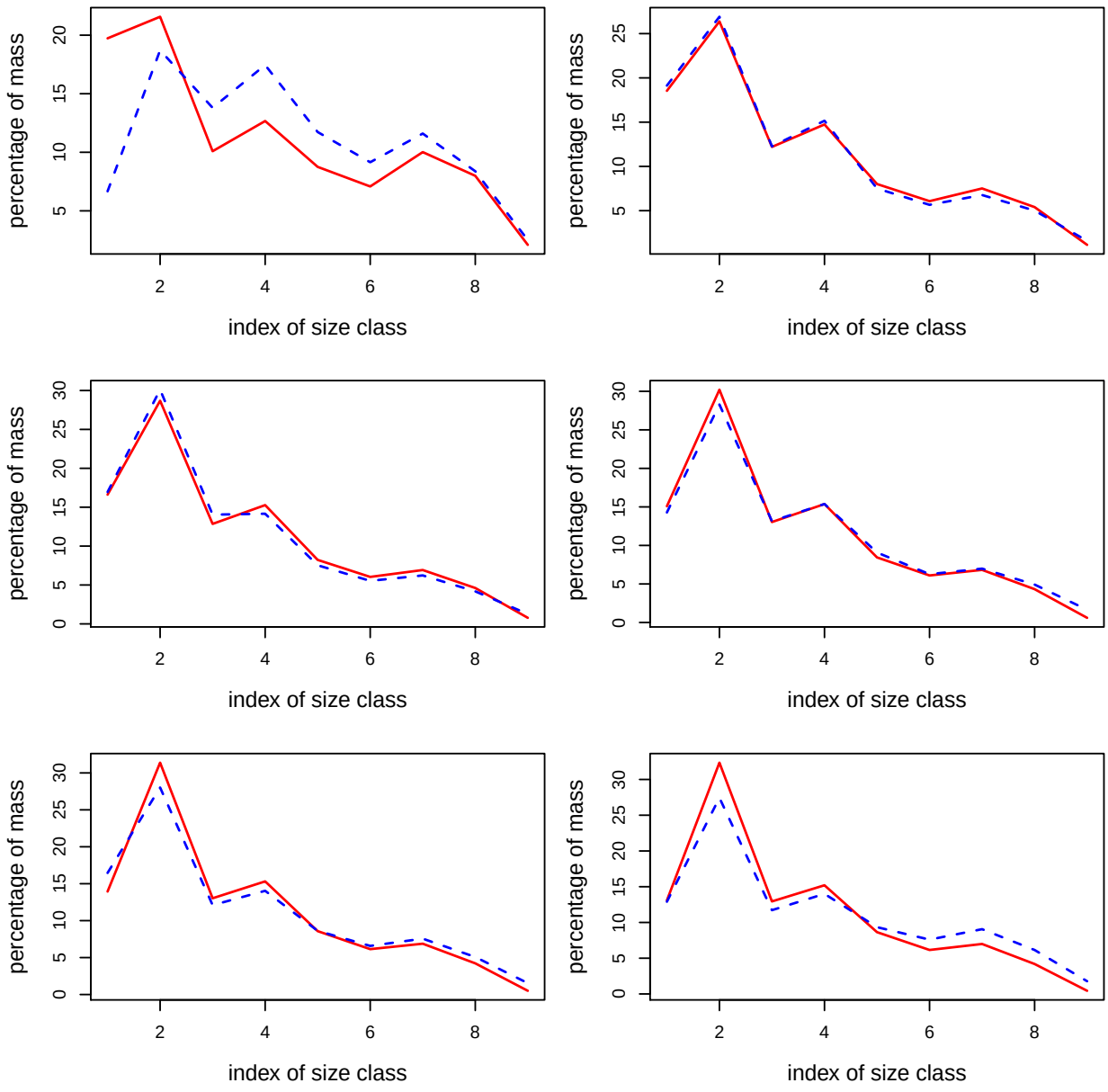

Figure 9: In-sample analysis for 4 mm grate size: observed data $\mathbf{m}_{out}^{obs}(k)$ (blue line) and model prediction $\mathbf{m}_{out}(k)$ (red line). Plots in each subfigure report the distributions for the 6 sampling intervals, by row, with increasing k from the top left to the bottom right corner.

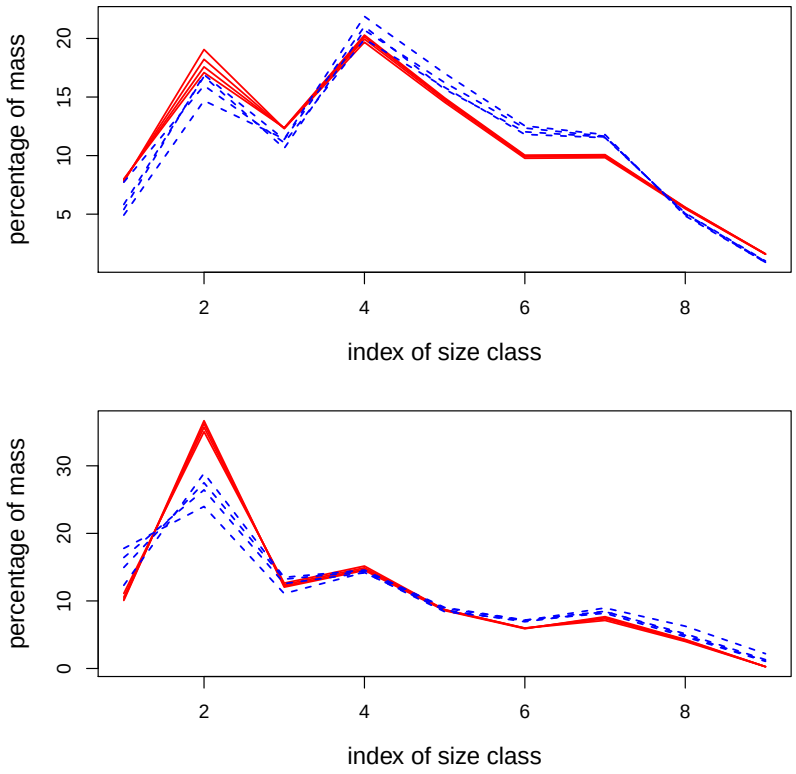

Figure 10: Out-of-sample validation for 2 mm (top) and 4 mm grate size (bottom) in the stationary state ($k = 8, \ldots, 11$): observed data $\mathbf{m}_{out}^{obs}(k)$ (blue lines) and model prediction $\mathbf{m}_{out}(k)$ (red lines). Each curve corresponds to a sampling interval from $k = 8$ to $k = 11$.

Results from the out-of-sample validation are reported in Figure 10 for the stationary state (sampling intervals from 8 to 11). They confirm the adherence between model and data in the stationary state.

Finally, the accuracy of the output size distribution prediction is quantified for the out-of-sample validation using the Kolmogorov-Smirnov metric (maximum distance between predicted and observed cumulated dimensional distribution in the stationary state). Results in Table 9 show that the metric is largely lower than 0.1 for all considered values of k, thus confirming the good adherence.

7. Conclusion

In this work, we have proved the effectiveness of PBMs for recycling, under appropriate simplifying assumptions that make it possible to use a constant set of parameters over a wide range of working conditions, thus enabling practical application.

		2 mm grate size	4 mm grate size
Out-of-sample	$k = 8$	0.043	0.072
	$k = 9$	0.052	0.059
	$k = 10$	0.042	0.053
	$k = 11$	0.064	0.049

Table 9: Kolmogorov-Smirnov metric for the out-of-sample validation in the stationary state ($k = 8, \ldots, 11$).

A wide experimental activity, focused on PCBs, has been conducted to confirm our ideas and validate the assumptions. PCBs are chosen for two reasons: first, they represent a relevant example of WEEE, as each modern electronic equipment includes PCBs and they include a high amount of precious metals and rare earths; second, the high variability of PCB features makes their recycling a very challenging task, which has not been effectively solved so far.

Experimental results confirmed that the assumptions are reasonable for the considered experimental layout. In particular, the multiplication assumption was not rejected and the saturation had only little effect, as a two-way ANOVA showed that Sat and v are never significant for levels below 25%, after applying the Bonferroni correction. The homogeneity assumption is tenable, except for the initial shredding period, as the null hypothesis of constant mean in every size class (while keeping the total shredding time fixed) was never rejected at the 5% significance level by an ANOVA test. Moreover, the accuracy of the predicted output size distribution was confirmed via an out-of-sample validation by the low values of the Kolmogorov-Smirnov metric, which are smaller than 0.1 for all the validation experiments. Finally, due to the general features of the process, it can be expected that the same simplified PBM is also valid for other machines and other PCB mixtures.

From the industrial point of view, our framework brings relevant advantages in everyday practice, reducing times and costs every time a new material or a new shredding machine needs to be characterized. Indeed, it will be possible to estimate the coefficients of the matrix $\mathbf{P}$ with a small number of experiments, and to keep their values constant over a wide range of working conditions.

Future work may be focused on extending the framework to other types of WEEE. Moreover, the impact of the initial transient phase of the comminution process on model

training could be examined, along with methods for reducing its effects. However, an explicit model of the transient phase is not of primary interest, as only the long-term behavior of the continuous comminution process is of practical industrial relevance.

Acknowledgements

This work is part of the Flagship Project "Factory of the Future – ZeroWastePCBs", coordinated by the National Research Council of Italy (CNR) and funded by the Italian Ministry of Education, University and Research (MIUR).

References

Austin, L., 1971. A review: introduction to the mathematical description of grinding as a rate process. Powder Technology 5, 1–17.

Bilgili, E., Capece, M., 2011. Quantitative analysis of multi-particle interactions during particle breakage: a discrete non-linear population balance framework. Powder technology 213, 162–173.

Bilgili, E., Scarlett, B., 2005. Population balance modeling of non-linear effects in milling processes. Powder Technology 153, 59–71.

Bizzo, W.A., Figueiredo, R.A., de Andrade, V.F., 2014. Characterization of printed circuit boards for metal and energy recovery after milling and mechanical separation. Materials 7, 4555–4566.

Braungart, M., McDonough, W., 2002. Cradle to Cradle: Remaking the Way We Make Things. North Point Press.

Broadbent, S., Calcott, T., 1956. A new analysis of coal breakage processes. Journal of the Institute of Fuel 29, 524–528.

Castro, M., Remmerswaal, J., Brezet, J., Schaik, A., Reuter, M., 2005. A simulation model of the comminution-liberation of recycling streams. relationships between product design and the liberation of materials during recycling. International Journal of Mineral Processing 75, 251–281.

Cesaro, A., Marra, A., Belgiorno, V., Guida, M., 2017. Effectiveness of weee mechanical treatment: Separation yields and recovered material toxicity. Journal of cleaner production 142, 2656–2662.

Colledani, M., Tolio, T., 2013. Integrated process and system modelling for the design of material recycling systems. CIRP Annals-Manufacturing Technology 62, 447–452.

Dehling, H.G., Gottschalk, T., Hoffmann, A.C., 2007. Stochastic modelling in process technology. volume 211. Elsevier.

Ellen Mac Arthur Foundation, 2013. Towards the circular economy. www.ellenmacarthurfoundation.org/assets/downloads/publications/Ellen-MacArthur-Foundation-Towards-the-Circular-Economy-vol.1.pdf, visited on Sept. 24, 2018.

Gaudin, A.M., 1939. Principles of mineral dressing. volume 351. McGraw-Hill New York.

Gay, S., 2004. A liberation model for comminution based on probability theory. Minerals Engineering 17, 525–534.

Gay, S., Wei, X., 1999. Liberation modelling using a dispersion equation. Minerals Engineering 12, 219–227.

Grübler, A., 2003. Technology and global change. Cambridge University Press: New York .

Gu, Y., Wu, Y., Xu, M., Mu, X., Zuo, T., 2016. Waste electrical and electronic equipment (weee) recycling for a sustainable resource supply in the electronics industry in china. Journal of Cleaner Production 127, 331–338.

King, R., 1979. A model for the quantitative estimation of mineral liberation by grinding. International Journal of Mineral Processing 6, 207–220.

King, R., Schneider, C., 1998. Mineral liberation and the batch comminution equation. Minerals Engineering 11, 1143–1160.

Menikpura, S., Santo, A., Hotta, Y., 2014. Assessing the climate co-benefits from waste electrical and electronic equipment (weee) recycling in japan. Journal of Cleaner Production 74, 183–190.

Nelen, D., Manshoven, S., Peeters, J.R., Vanegas, P., D'Haese, N., Vrancken, K., 2014. A multidimensional indicator set to assess the benefits of weee material recycling. Journal of Cleaner Production 83, 305–316.

Oliveira, P., Taborda, F., Nogueira, C., Magarido, F., 2013. The effect of shredding and particle size in physical and chemical processing of printed cicuit boards waste, in: Materials Science Forum, Trans Tech Publ. pp. 653–658.

Ongondo, F.O., Williams, I.D., Cherrett, T.J., 2011. How are weee doing? a global review of the management of electrical and electronic wastes. Waste management 31, 714–730.

Parajuly, K., Wenzel, H., 2017. Potential for circular economy in household weee management. Journal of Cleaner Production 151, 272–285.

Pearce, D.W., Turner, R.K., 1989. Economics of Natural Resourcing and the Environment. Johns Hopkins University Press.

Picone, N., Colledani, M., Copani, G., Diani, M., Tolio, T., 2016. Towards smart e-waste demanufacturing systems exploiting cyber-physical systems (cpss) capabilities, in: Proceeding of Electronics Goes Green Conference, September 2016.

R Core Team, 2014. R: A Language and Environment for Statistical Computing. R Foundation for Statistical Computing. Vienna, Austria.

Schaik, A.V., Reuter, M., 2010. Dynamic modelling of e-waste recycling system performance based on product design. Minerals Engineering 23, 192–210.

Schaik, A.V., Reuter, M., Heiskanen, K., 2004. The influence of particle size reduction and liberation on the recycling rate of end-of-life vehicles. Minerals Engineering 17, 331–347.

Sedlatschek, K., Bass, L., 1953. Contribution to the theory of milling processes. Powder Metallurgy 6, 148–153.

Veroux, A., Grotti, D., 2010. Modeling and optimization of a multi-stage shredding-separation systems for recycling. Master Thesis in Industrial Engineering, Politecnico di Milano, Milan, Italy, Dec. 21th, 2010. http://hdl.handle.net/10589/10762.

website of STIIMA, . Re/de-manufacturing pilot plant. www.stiima.cnr.it/it/index.php?sez=10&ssez=3, visited on Sept. 24, 2018.

Wortmann, A., Combemale, B., Barais, O., 2017. A systematic mapping study on modeling for industry 4.0, in: Proceedings of the ACM/IEEE 20th International Conference on Model Driven Engineering Languages and Systems (MODELS), pp. 281–291.

Zlamparet, G.I., Ijomah, W., Miao, Y., Awasthi, A.K., Zeng, X., Li, J., 2017. Remanufacturing strategies: A solution for weee problem. Journal of Cleaner Production 149, 126–136.

Appendix: notation and abbreviation list

- ANOVA: Analysis of Variance
- B_{ijt}: breakage parameter from class i to class j in the interval $[t, t + \Delta]$
- d_{iit}: mass fraction in class i that leaves the chamber in the interval $[t - \Delta, t]$
- $\mathbf{D_t}$: diagonal discharge matrix containing d_{iit} $(i = 1, \ldots, n)$
- $\mathbf{D}$: homogeneous discharge matrix
- Δ: breakage interval
- $\mathbf{I}$: identity matrix
- k: number of breakage intervals
- $m_i(t)$: overall mass of particles in class i at time t
- $\mathbf{m}(t)$: mass vector containing $m_i(t)$ $(i = 1, \ldots, n)$
- $\mathbf{m}(k)$: mass vector $\mathbf{m}(t)$ indexed by the number k of breakage events
- $\mathbf{m}_{ch}(t)$: vector of the mass remaining in the chamber at time t
- $\mathbf{m}_{in}(t)$: vector of input mass refilled at time t
- $\mathbf{m}_{out}(t)$: vector of mass discharged in the interval $[t - \Delta, t]$
- $\mathbf{m}_{out}^{obs}(k)$: mass vector m_{out} experimentally observed at k
- m_{sat}: mass at $Sat = 100\%$
- n: number of size classes
- N: number of rotor blades
- p_{ijt}: mass fraction moving from class i to class j in the interval $[t, t + \Delta]$

- $\mathbf{P_t}$: breakage matrix containing p_{ijt} $(i = 1, \ldots, n;\ j = 1, \ldots, n)$
- $\mathbf{P_k}$: breakage matrix $\mathbf{P_t}$ indexed by the number k of breakage events
- $\mathbf{P}$: homogeneous breakage matrix
- PBM: Population Balance Model
- PCB: Printed Circuit Board
- q_{ii}^d: logit of probability d_{ii}
- q_{ij}^p: logit of probability p_{ij}
- Sat: chamber saturation
- S_{it}: selection rate for class i in the interval $[t, t + \Delta]$
- t: time
- v: rotor speed
- V: chamber volume
- WEEE: Waste Electrical and Electronic Equipment
- ρ: density of the particle mix
- σ: shredding time
- τ: shredding time
- *: statistical significance (in Table 6)